Formation and Contraction of a Microfilamentous Shell in Saponin-permeabilized Platelets

Freddy Stark, Rajasree Golla, and Vivianne T. Nachmias

Department of Anatomy, University of Pennsylvania School of Medicine, Philadelphia, Pennsylvania 19104-6058

Abstract. To study the mechanism of granule centralization in platelets, we permeabilized with saponin in either EGTA (5 mM) or calcium (1 or 10 μM). Under all conditions, platelets retained 40–50% of their total actin and >70% of their actin-binding protein (ABP) but lost >80% of talin and myosin to the supernatant. Thin sections of platelets permeabilized in EGTA showed a microfilament network under the residual plasma membrane and throughout the cytoplasm. Platelets permeabilized in calcium contained a microfilament shell partly separated from the residual membrane. The shell stained brightly for F-actin. A less dense microfilament shell was also seen in sections of ADP-stimulated intact platelets subsequently permeabilized in EGTA.

In the presence of 1 mM ATPγS and calcium, myosin was retained (70%) and was localized by indirect immunofluorescence in bright central spots that also stained intensely for F-actin. Electron micrographs showed centralized granules surrounded by a closely packed mass of microfilaments much like the structures seen in thrombin-stimulated intact platelets subsequently permeabilized in EGTA. Permeabilization in calcium, ATP, and okadaic acid, produced the same configuration of centralized granules and packed microfilaments; myosin was retained and the myosin regulatory light chain became phosphorylated. Microtubule coil disassembly before permeabilization did not inhibit granule centralization.

These results suggest a possible mechanism for granule centralization in these models. The cytoskeletal network first separates from some of its connections to the plasma membrane by a calcium-dependent mechanism not involving ABP proteolysis. Phosphorylated myosin interacts with the microfilaments to contract the shell moving the granules to the platelet's center.

RESTING discoid platelets, when stimulated by various agonists, rapidly undergo striking changes in shape and structure. This makes them very useful subjects for the study of the relationship of these changes to the underlying cytoskeleton.

A major cytoskeletal feature in resting platelets is a continuous circumferential microtubule coil (Nachmias et al., 1979; Kenney and Linck, 1985). The remaining cytoplasm is dense, and electron micrographs reveal little cytoskeletal detail. The secretory granules are randomly scattered throughout the cytoplasm. To see more cytoskeletal detail in resting platelets, Boyles used simultaneous extraction and fixation. This preparation showed a network consisting of submembranous and cytoplasmic microfilaments (Fox et al., 1984).

Upon addition of an agonist, internal calcium levels rise and platelets rapidly change shape (Yoshida et al., 1986, 1988). If the stimulus is strong, as with thrombin, electron micrographs show that the granules are gathered into the center and are surrounded by a dense mass of microfilaments. The microfilaments are themselves surrounded by tightly coiled microtubules. This centralization is typical of the secretory process in human platelets (Gerrard and White, 1976).

In this study, we used controlled permeabilization to obtain more information about cytoskeletal structure in the resting platelet and to study the effects of elevating calcium upon this structure, bypassing agonist action entirely. We were stimulated by the work of Brass and Joseph (1985) who showed that low levels of saponin allowed the entry of small molecules and ions into platelets. We previously found after using a higher saponin level that a distinct and reproducible set of proteins were found in the supernatant while a different set remained associated with the platelets (Yoshida and Nachmias, 1987). This suggested that the preparation would be useful for further study.

To avoid secondary activation, we (*a*) pretreated the platelet suspensions with indomethacin to block thromboxane synthesis (Authi et al., 1986); (*b*) included phosphocreatine and creatine phosphokinase in the permeabilization buffer to exclude activation by ADP; and (*c*) fixed the permeabilized platelets in suspension to eliminate activation due to centrifuging. Our observations clearly show that directly exposing the platelet interior to micromolar calcium in the absence

This work was presented at the joint ASCB/ASBMB meeting in San Francisco, 1989.

of agonist causes structural changes in the platelet cytoskeleton that mimic the changes produced by agonists.

Materials and Methods

Materials

ADP, anti-tubulin antibody, apyrase, ATP, colcemid (demecolcine), creatine phosphokinase, DNA (type 1), DNase I, hirudin, H_2O_2, indomethacin, leupeptin, PMSF, phosphocreatine, poly-L-lysine, saponin, and thrombin were obtained from Sigma Chemical Co. (St. Louis, MO).

Preparation of Platelets

Platelets were prepared as previously described (Yoshida et al., 1988) with the following modifications: while the platelets were suspended in the Pipes buffer (10 mM Pipes, 140 mM NaCl, 2.7 mM KCl, 5.5 mM glucose, and 0.1 mg/ml apyrase, pH 6.5), 25 μM indomethacin was added and the platelets were incubated at 37°C in this buffer for 30–45 min; subsequently, the platelet suspension was centrifuged at 400 *g* for 10 min and the pelleted platelets were resuspended in high KCl buffer (5 mM Hepes, 140 mM KCl, 2.7 mM NaCl, 12 mM NaH_2PO_4, 5 mM $MgCl_2$, 5.5 mM glucose, 5 mM phosphocreatine, 10 U/ml creatine phosphokinase, and 100 μg/ml leupeptin, pH 7.1). The high KCl buffer included 5 mM EGTA, 1 or 10 μM free calcium. Free calcium in a Ca^{2+}/EGTA buffer was calculated by the program of Chantler et al. (1981). Phosphocreatine and creatine phosphokinase were omitted when 1 mM ATPγS (tetralithium salt; Boehringer Mannheim Biochemicals, Germany) was used. We exposed some platelets suspended in KCl buffer with 10 mM EGTA to 0.5 U/ml of thrombin for 1 min before permeabilization with saponin. Thrombin activity was stopped by the addition of 1 unit/ml of hirudin, 2 mM PMSF, and 200 μM leupeptin before saponin addition. Control experiments were performed with leupeptin added before thrombin to block the effect of thrombin. We activated other platelets with 20 μM ADP in 5 mM EGTA before permeabilization. After 20 s, ADP was converted to ATP by the addition of phosphocreatine and creatine phosphokinase simultaneously with saponin.

Analysis of Platelet Fractions

At various times after saponin permeabilization, 100 μl of the platelet suspension was centrifuged at ~9,500 *g* in a microfuge B (Beckman Instruments, Fullerton, CA) for 50 s. Samples were prepared for SDS-PAGE as previously described (Yoshida and Nachmias, 1987); the supernatants were pipetted off and sample buffer added to the cell pellet and supernatant fractions. Bands on the 10% Coomassie blue-stained gels were measured with a scanning densitometer (Dr. J. Haselgrove, University of Pennsylvania).

Supernatant fractions were assayed for G-actin by their ability to inhibit DNase I with a scaled down modification of the method of Fox and colleagues (1981). The DNAse I concentration was increased to 1 KIU/ml and 0.45 ml of DNA was used in microcuvettes. As a result, initial rates were linear. Only inhibitions in the 30–70% range were used.

Fluorescence and Electron Microscopy

15 min after permeabilization, platelet suspensions were fixed by the addition of one-tenth volume of freshly prepared 10% formaldehyde. For fluorescence microscopy, the platelets were allowed to settle onto poly-L-lysine-coated coverslips, permeabilized with −20°C methanol and stained with rhodamine-labeled phalloidin (Molecular Probes, Inc., Eugene, OR) or exposed to affinity-purified rabbit anti-human platelet myosin antibody prepared in our laboratory followed by fluorescein-labeled goat anti-rabbit $F(ab')_2$ (Tago, Inc., Burlingame, CA) presorbed with fixed platelets. Indirect immunofluorescence microscopy with anti-tubulin antibody was used to confirm the disassembly of the microtubule coil after chilling and colcemid treatment. For photography, we used a Zeiss research microscope equipped for epifluorescence, a 100× Olympus objective, NA 1.30, and T-Max 100 film (Eastman Kodak Co., Rochester, NY).

For whole-mount EM, formaldehyde-fixed platelets were allowed to settle onto carbon-coated grids. The grids were rinsed with KCl buffer then with buffer containing 0.5% Triton X-100 (J. T. Baker Chemical Co., Phillipsburg, NJ). The remaining structures were fixed in 0.2 M glutaraldehyde in 0.1 M sodium cacodylate buffer, pH 7.3, for 5 min followed by 30 s in 1% osmium tetroxide in 0.1 M sodium cacodylate buffer, pH 7.3.

Permeabilized platelets were prepared for thin sectioning by a modification of the method of J. Boyles (Fox et al., 1984) deleting Triton X-100. The platelet suspension was fixed by adding an equal volume of 0.4 M glutaraldehyde, 80 mM lysine, and 0.1 M sodium cacodylate, pH 7.3, at room temperature for 1 h. The suspension was centrifuged, and the cell pellet was rinsed three times with 0.1 M sodium cacodylate, pH 7.3. A brief postfixation followed with cold 1% osmium tetroxide in 0.1 M sodium cacodylate buffer, pH 7.3, for 10 min on ice. The cell pellet was quickly rinsed with cold distilled water and stained overnight, en bloc, at room temperature with 1% aqueous uranyl acetate. The pellets were dehydrated with a graded ethanol series, infiltrated, embedded in Spurr's resin and thin-

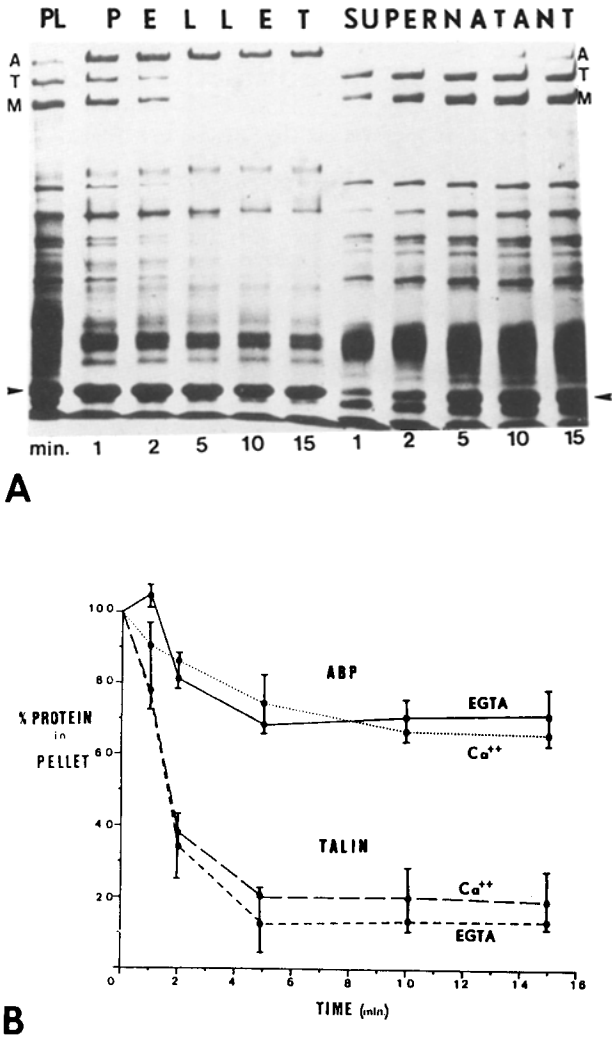

Figure 1. (*A*) A 7.5% SDS-polyacrylamide gel of permeabilized platelet pellet and supernatant fractions in 1 μM free Ca^{2+}. The pellet (cellular) and supernatant fractions were separated at 1, 2, 5, 10, or 15 min after saponin addition. Note the loss of talin (*T*: 235 kD) and myosin (*M*: 200 kD) and about half of the 42-kD band (actin; *arrow*) from the cellular fraction and their appearance in the supernatant fractions, and by contrast, the retention of actin-binding protein (*A*: 250 kD). Platelets permeabilized in either 5 mM EGTA or 10 μM free Ca^{2+} yielded similar results. Lane *PL* is whole platelet lysate. (*B*) Graph of densitometric scans of polyacrylamide gels of platelet cellular fractions showing loss of talin and actin-binding protein with time. About 70–75% of the actin-binding protein remains 15 min after permeabilization, whereas only 10–20% of talin remains. Each point represents the mean of four different experiments ± SD. Due to similarities in results, the data from gels of platelets permeabilized in 1 and 10 μM calcium were pooled.

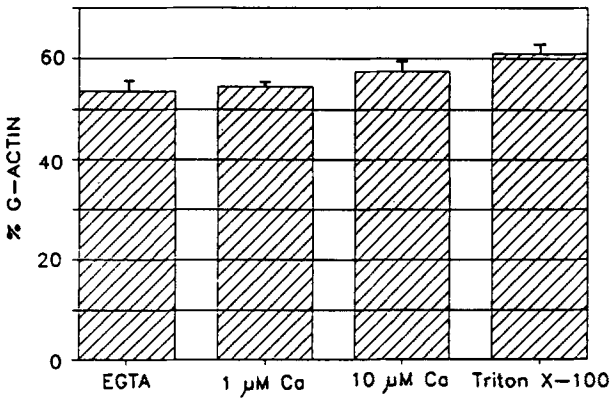

Figure 2. DNase I inhibition assay for G-actin in the supernatants of saponin-permeabilized platelets. Results are of a typical experiment. Each assay was repeated three times, and the results are the mean + SD. Triton X-100-treated platelets were used as a control for total G-actin. Total platelet actin was determined using platelets treated with Triton X-100 in guanidine buffer (see Materials and Methods).

sectioned. Sections were stained with lead, and the specimens were viewed with a Phillips 201 electron microscope operating at 80 kV.

Immunoblotting

Whole platelet lysate, prepared as previously described (Yoshida and Nachmias, 1987), was electrophoresed on a 7.5% polyacrylamide gel, the proteins transferred to nitrocellulose (Towbin et al., 1979), blocked with BSA and exposed to the affinity-purified anti-platelet myosin antibody. After incubation with goat-anti-rabbit peroxidase-conjugated $F(ab')_2$ fragment (Cappel Laboratories, West Chester, PA), the immunoblot was developed with diaminobenzidine (Polysciences, Inc., Warrington, PA) and H_2O_2.

Phosphorylation and Autoradiography

Platelets suspended in Pipes buffer were incubated with 1 mCi/ml $H_3[^{32}P]O_4$ (ICN Radiochemicals, Irvine, CA) for 1 h at 37°C. The platelets were then centrifuged and resuspended in the high KCl buffer as described above. Just before the addition of saponin, 0.25 mCi/ml ATP-γ-^{32}P (ICN Radiochemicals, Irvine, CA) without or with 10 μM okadaic acid (a gift from Dr. A. V. Somlyo, University of Virginia) was added and phosphocreatine and creatine kinase were omitted. Platelets were permeabilized for 15 min, centrifuged, and separated into cellular and supernatant fractions. As controls, intact resting platelets and intact platelets exposed to 0.25 U/ml thrombin for 1 min were used. Sample buffer was added to the fractions and controls, and the samples were electrophoresed on 13% polyacrylamide gels. Stained, dried gels were exposed to X-Omat AR film (Eastman Kodak Co.) at −80°C with Dupont Cronex lightning screens.

Results

Cytoskeletal Proteins in Permeabilized Platelets

Fig. 1 *A* is an SDS-polyacrylamide gel of aliquots of the separated pellet (cellular) and supernatant fractions of platelets at times after permeabilization in 1 μM calcium. Four major cytoskeletal proteins identified are ABP (250 kD; Rosenberg et al., 1981), talin (235 kD; O'Halloran et al., 1985), myosin (200-kD heavy chain; Pollard et al., 1974) and actin. While much of the ABP remains with the cellular fraction during the 15 min sampled, most of the myosin and talin diffuse into the supernatant. This difference in retention was seen whether the cells were permeabilized in the presence of 5 mM EGTA, in 1 or 10 μM calcium. We also observed that about half of the 42-kD band (actin) was lost to the supernatant under all three conditions. Fig. 1 *B* shows a quantitative analysis of the time course of protein retention. After 15 min, 80% of the talin is lost, whereas 70% of ABP is retained. The retention curves are similar whether the platelets are permeabilized in micromolar calcium or in EGTA. ABP was not proteolyzed in micromolar calcium (see Fig. 1 *A*). Myosin retention will be discussed later.

As noted above, actin (42 kD) also appears in the supernatant. Fig. 2 shows the results of a DNase I inhibition assay for G-actin of platelets permeabilized for 15 min. The supernatants contained between 53.6 and 57.4% of the total actin. This actin is in monomer form since supernatants treated with guanidine yielded the same values (data not shown). The amount of actin diffusing out almost equals the level found in the supernatant of platelets permeabilized with Triton X-100 (61% G-actin). There is a slight increase in G-actin in the supernatants of platelets permeabilized in 10 μM calcium, but, on the whole, the percentage of G-actin diffusing out of the permeabilized cells is 87.9–94.1% of that of the Triton extracts.

Structure of Saponin-permeabilized Platelets

Fig. 3 *A* is an electron micrograph of a thin section of a typical platelet permeabilized in EGTA. Platelets treated in this manner exhibit a microfilament network extending well into the cytoplasm, under the plasma membrane and between the granules. Fig. 3 *B* is a magnified view showing a microfilamentous network directly underneath the remaining plasma membrane. However, when platelets were permeabilized in 1 or 10 μM free calcium, the structure looked very different. Fig. 3, *C–E* show different views of the circumferential microfilament ring which form under these conditions. These rings (*arrows*) are 0.1–0.3 μm wide. The micrographs show that the circumferential microfilaments may be close to (Fig. 3 *C*) or more separated from (Fig. 3, *D* and *E*) the remaining membrane.

Compare Fig. 3, *C–E* with Fig. 4, which shows the structure of platelets exposed to 20 μM ADP in 5 mM EGTA for 15 s before permeabilization (see Materials and Methods). The ADP-stimulated platelets also exhibit circumferential microfilaments surrounding the granules. The three micrographs in Fig. 4 show a hypothetical progression in increased density and decreased diameter of this circumferential ring. Platelets permeabilized in micromolar calcium typically have denser microfilament rings which have pulled further away from the remaining plasma membrane than those stimulated with ADP (compare Fig. 3, *C–E* with Fig. 4, *A–C*).

Retention of Myosin and its Effect on the Cytoskeletal Structure

When phosphorylated on the regulatory light chain by a calcium-calmodulin dependent kinase (Dabrowska and Hartshorne, 1978; Hathaway and Adelstein, 1979), myosin can interact with and be activated by F-actin (Adelstein and Conti, 1975). Myosin might, therefore, be retained in platelets permeabilized in micromolar calcium due to its interaction with microfilaments, but, in fact, it does not remain in the cellular fraction (Fig. 1 *A*). Since phosphorylation could be rapidly followed by dephosphorylation, we included 1 mM

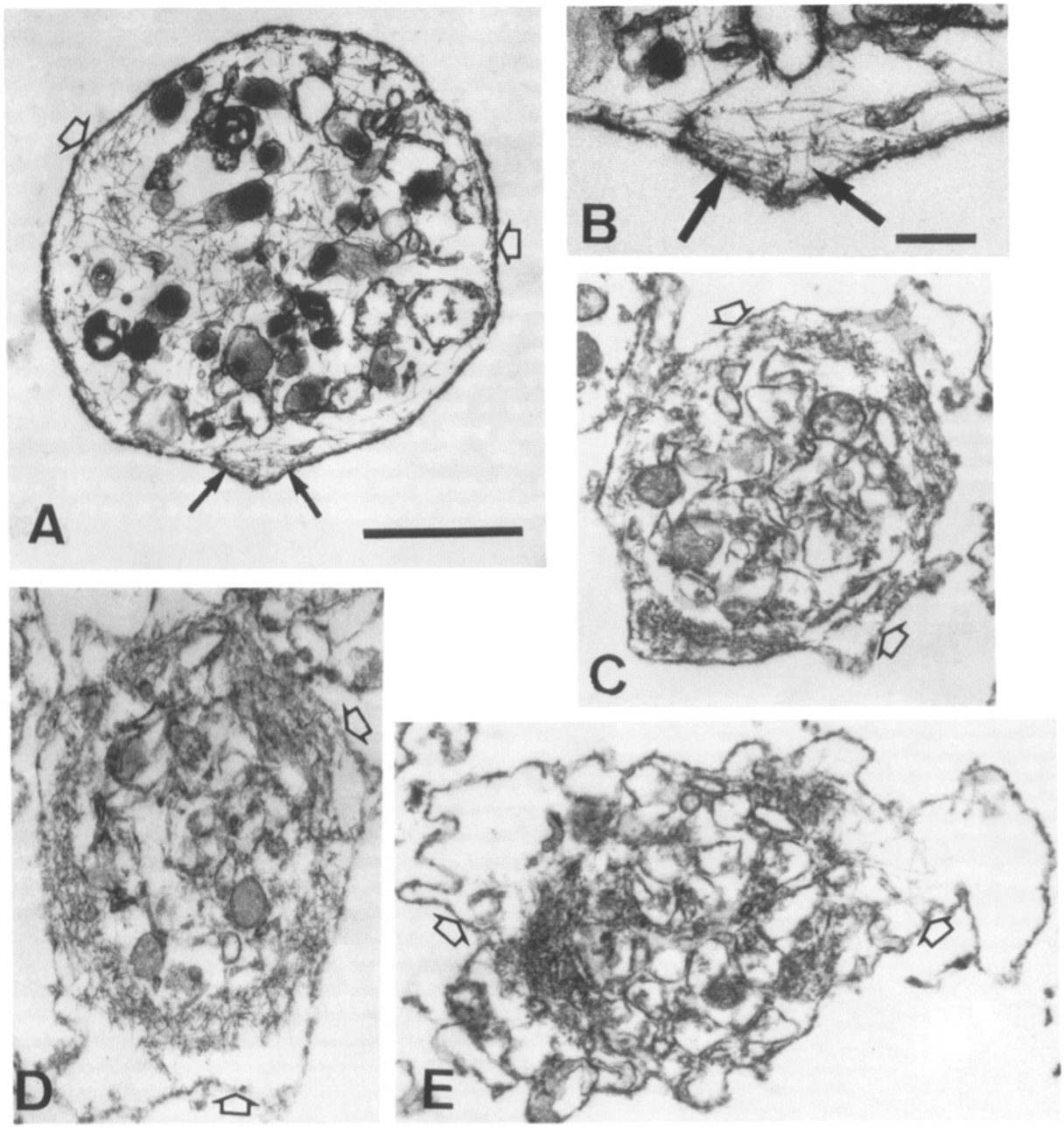

Figure 3. Micrographs of platelets permeabilized in buffer containing 5 mM EGTA (*A* and *B*) or 1 μM free Ca^{2+} (*C–E*). *A* is a thin section of a platelet permeabilized in EGTA showing microfilaments traversing the cytoplasm and underneath the remaining plasma membrane (*solid arrows*). *B* shows a more magnified view of the subplasmalemmal microfilament (*arrows*). *C–E* show platelets permeabilized in 1 μM free Ca^{2+}. This series of micrographs show a hypothetical progression of the separation of the microfilament shell from the remaining membrane in micromolar calcium. The clear arrows point to the remaining plasma membrane. Bar: (*A*) 1 μm; (*B*) 0.1 μm.

ATPγS. This ATP analogue can be used by the kinase to phosphorylate myosin regulatory light chain, but the thiophosphate group is not removed by myosin light chain phosphatase (Morgan et al., 1976).

Fig. 5 *A* shows that myosin is retained in platelets permeabilized in the presence of both ATPγS and micromolar calcium. The densitometric tracings of Fig. 5 *C* show that the effect is specific: ~70% of the myosin is retained in micromolar calcium with ATPγS, whereas in micromolar calcium alone or in EGTA with or without ATPγS >80% of myosin is lost from the cells. More than 80% of the talin still diffuses out under all conditions (Fig. 5 *B*; Fig. 1), whereas >80% of the actin-binding protein remains in the platelet throughout as in preparations without ATPγS (Fig. 1).

Thin sections show no difference in the structure of platelets permeabilized in EGTA and ATPγS as compared to EGTA alone (data not shown). When both micromolar calcium and ATPγS are present, there is a striking change. Fig. 6 *B* shows a section of platelets permeabilized in 10 μM calcium and ATPγS. Fig. 6 *A* is a comparable thin section of intact platelets that were thrombin-stimulated and then permeabilized in EGTA. Both micrographs show that the plate-

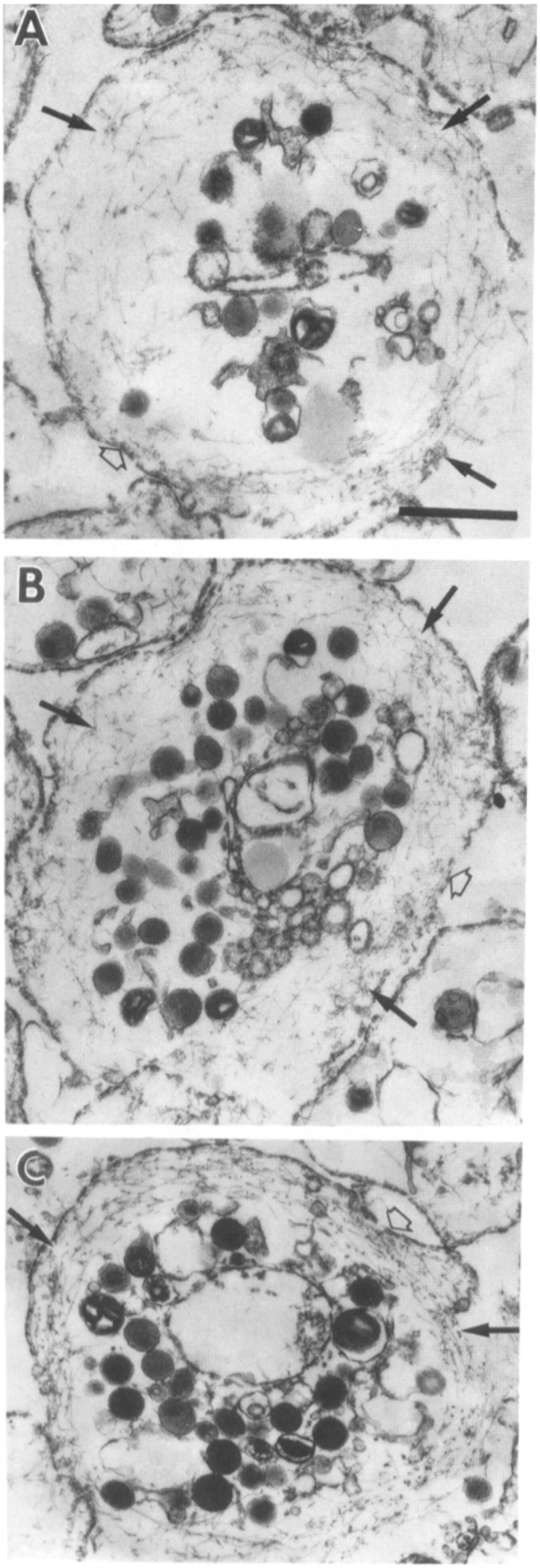

lets now contain a compact microfilament shell surrounding closely packed granules (*solid arrows*) with a considerable space between the shell and the remaining membrane. The microfilament shells of these platelets are half the size of platelets permeabilized in micromolar calcium alone (Fig. 3, *C–E*). Note that the microfilament shell of platelets permeabilized in calcium and ATPγS contracts around the granules in the absence of ABP proteolysis.

Two slight differences between the thrombin-treated platelets and platelets permeabilized in micromolar calcium and ATPS were consistently seen. First, the microfilament shells of the thrombin-stimulated platelets are more compact and rounded as compared with the microfilament shells of platelets permeabilized in micromolar calcium and ATPγS, and second, some of the granules in the thrombin-stimulated platelets are electron-lucent, indicating loss of their contents, presumably by secretion.

To compare the distribution of F-actin and myosin in the permeabilized platelets, we used rhodamine-phalloidin staining for F-actin and an affinity-purified antibody to platelet myosin. Fig. 7 displays a gallery of photomicrographs which show that with rhodamine-phalloidin: (*a*) platelets permeabilized in the presence of EGTA with or without ATPγS stain fairly evenly with strands of fluorescence (Fig. 7 *A*); (*b*) platelets permeabilized in micromolar calcium alone show arcs or rings of staining (Fig. 7 *B*); (*c*) platelets permeabilized in EGTA after thrombin show bright, central fluorescent spots surrounded by a lighter staining peripheral region (Fig. 7 *C*); (*d*) when permeabilized in the presence of ATPγS and EGTA (Fig. 7 *D*), the platelets show diffuse staining similar to platelets permeabilized in EGTA alone; and (*e*) platelets permeabilized in ATPγS and micromolar calcium (Fig. 7 *E*) show a bright, central fluorescent spot very similar to the thrombin treated platelets (Fig. 7 *C*).

With the affinity-purified anti-myosin, ~90% of the platelets permeabilized in EGTA with ATPγS show very weak staining at background levels (Fig. 7 *F*); but in platelets permeabilized in micromolar calcium and ATPγS there are small spots of bright fluorescence (Fig. 7 *G*). These findings suggest that in the presence of micromolar calcium and ATPγS the shell of microfilaments, which contains both actin and myosin, has contracted down to the dimensions of a bright central spot. The presence of the very weak signal in platelets permeabilized in EGTA (Fig. 7 *F*) or in calcium alone (not shown) agrees with the polyacrylamide gel data (Fig. 5 *C*) that show a loss of >85% of the myosin under these conditions. Fig. 7 *H* shows the specificity of the antibody for myosin. The combination of calcium and ATPγS centralizes granules in >90% of permeabilized platelets as shown in Fig. 8 *A* and confirmed by immunofluorescence.

A second way of inhibiting dephosphorylation is by the use

Figure 4. Thin-section electron micrographs of platelets treated with 20 μm ADP for 15 s in 5 mM EGTA and subsequently permeabilized in EGTA (see Materials and Methods). *A* shows the circumferential microfilaments (*solid arrows*) just forming at the platelet's periphery. *B* shows an intermediate state, whereas *C* shows the microfilaments in a more contracted state (*solid arrows*) around the platelet's granules. The clear arrows point to the remaining plasma membrane. Bar, 1 μm.

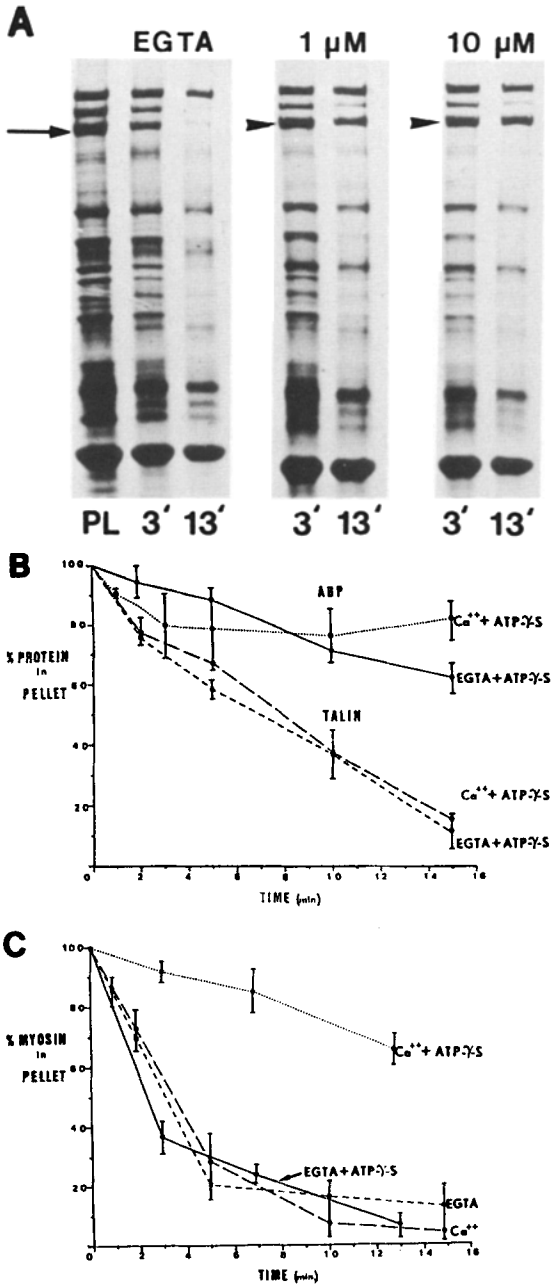

Figure 5. (*A*) A 7.5% polyacrylamide gel of the cellular fraction of platelets permeabilized in the presence of 1 mM ATPγS with either 5 mM EGTA, 1 or 10 μM free calcium. Note the retention of myosin (*arrowheads*) in the calcium treated samples. The graphs represent scans of four samples per time point ± the standard deviation. *B* shows ABP retention and talin loss in the cellular fraction of platelets permeabilized in either micromolar calcium or 5 mM EGTA in the presence of 1 mM ATPγS. Note that talin is lost at a slower rate than from platelets permeabilized in the absence of ATPγS (see Fig. 1 *B*). *C* shows myosin retention in the cellular fraction of platelets permeabilized in either micromolar calcium or 5 mM EGTA with or without 1 mM ATPγS. Due to similarities in results, the data from gels of platelets permeabilized in either 1 or 10 μM calcium were pooled.

of a phosphatase inhibitor. Okadaic acid strongly inhibits myosin light chain phosphatase and enhances tension development in Triton X-100-skinned smooth muscle fibers (Biajolian et al., 1988). We used okadaic acid in permeabilized platelet preparations to see if it would have an effect similar to that of ATPγS. Indeed, Fig. 8 *A* shows that more than 85% of the platelets permeabilized in the presence of 10 μM okadaic acid and micromolar calcium also have centralized granules.

Platelets permeabilized in micromolar calcium with either ATPγS (Fig. 8 *B*) or okadaic acid (Fig. 8 *C*) both contain

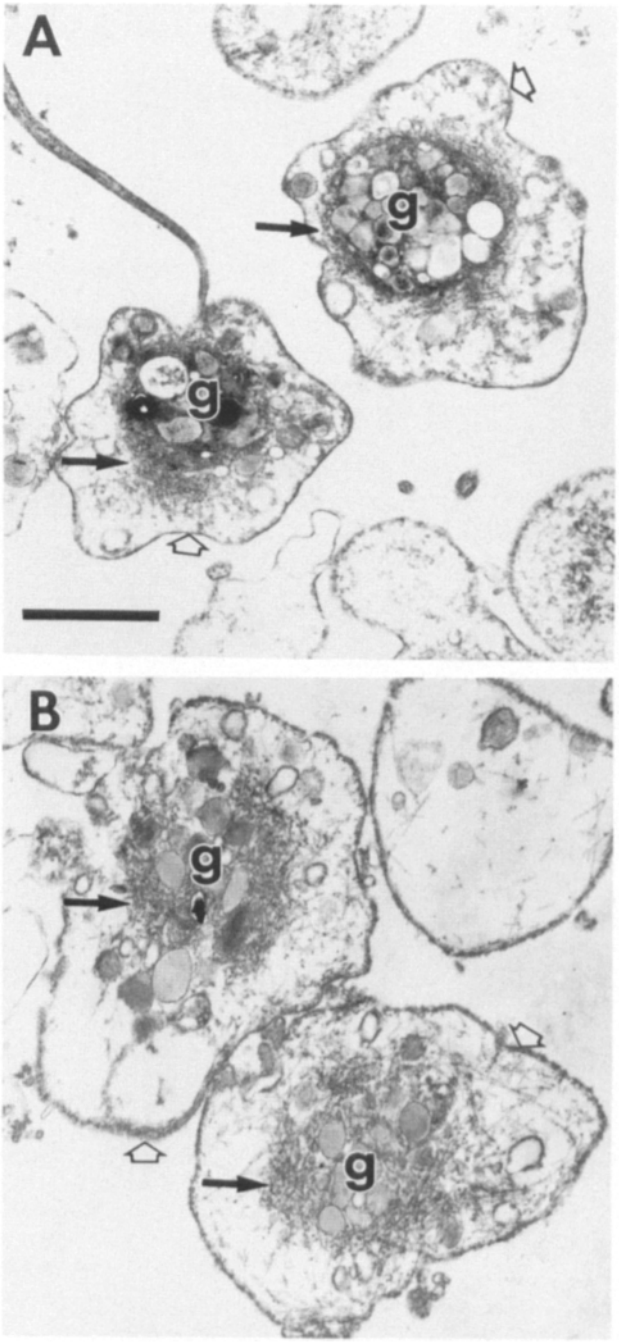

Figure 6. Thin-section electron micrographs of platelets permeabilized under two different conditions. *A* shows platelets that were treated with 0.5 units/ml thrombin and then permeabilized in 5 mM EGTA (see Materials and Methods). *B* shows platelets permeabilized in 10 μM calcium and 1 mM ATPγS. Note the centralized granules (*g*) surrounded by a condensed shell of microfilaments (*solid arrows*) in each of these micrographs. The clear arrows point to the remaining plasma membrane. Bar, 1 μm.

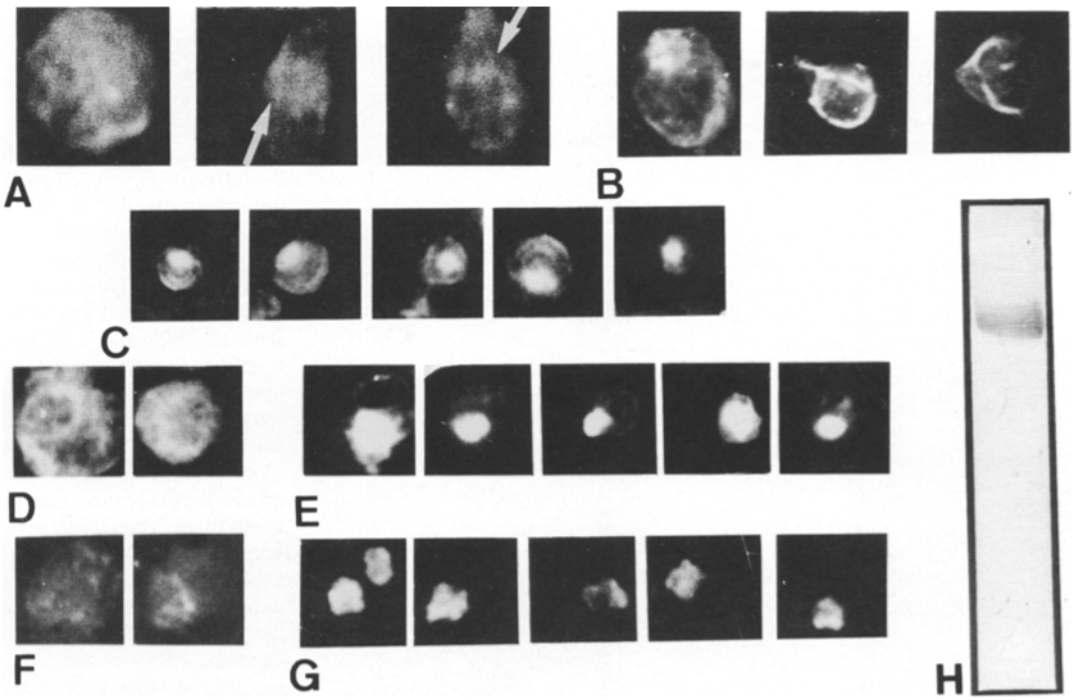

Figure 7. Gallery of fluorescence micrographs of permeabilized platelets. In Panel A, platelets were permeabilized in 5 mM EGTA, fixed and stained with rhodamine-phalloidin. Note the even staining and the strand-like structures in two of the platelets (*arrows*). In *B*, platelets were permeabilized in either 1 or 10 μM calcium, fixed and stained with rhodamine phalloidin. Note the presence of brightly stained arcs or rings. *C* shows rhodamine phalloidin staining of platelets treated with thrombin before permeabilization in 5 mM EGTA. Note the bright spot of staining with light staining peripherally. *D* shows platelets permeabilized in 5 mM EGTA with 1 mM ATPγS and stained with rhodamine phalloidin. Note the similarity to *A*. *E* shows platelets permeabilized in 10 μM calcium with ATPγS and stained with rhodamine phalloidin. Note the bright spot of staining and the similarity to the thrombin-treated platelets in *C*. F shows platelets permeabilized in EGTA with ATPγS and indirectly stained with affinity-purified anti-platelet myosin antibody. Note the very light staining pattern which agrees well with the polyacrylamide gel data of Fig. 7. *G* shows indirect myosin immunofluorescence of platelets permeabilized in 10 μM calcium with ATPγS. Note that the staining is in the form of bright, irregular spots about the same size as the rhodamine-phalloidin stained spots (*E*). All of the micrographs are 1750 X. *H* is an immunoblot of the affinity-purified anti-platelet myosin staining of whole platelet lysate (the polyacrylamide gel pattern of whole platelet lysate can be seen in Figs. 1 *A* and 7 *A*).

dense, amorphous masses with centrally located granules with a few microfilaments visible near the periphery. To see if the microtubule coil played a role in the granule centralization, we pretreated platelets with cold and colcemid before permeabilization as described. Fig. 8 *A* shows that the disassembly of the coil did not inhibit granule centralization in platelets permeabilized in micromolar calcium and ATPγS.

Fig. 9 shows that myosin light chain is phosphorylated in platelets permeabilized in micromolar calcium and okadaic acid. Lane *1* shows a band with the mobility of myosin light chain (M_r 20,000) phosphorylated in the cellular fraction of of ^{32}P-labeled platelets permeabilized in micromolar calcium and 10 μM okadaic acid. Note that this band is also heavily phosphorylated in platelets treated with thrombin (lane *Th*). The band is not present in the supernatant fraction (lane *2*). ^{32}P-labeled platelets permeabilized in 10 μM free calcium without okadaic acid or in EGTA with okadaic acid (which do not centralize their granules) show no phosphorylation of the light chain in either the cellular or supernatant fractions (lanes *3–6*). Resting platelets incubated with ^{32}P show only a low background level of light chain phosphorylation (lane *R*). Therefore, phosphorylation of the light chain correlates with granule centralization.

Discussion

Calcium is strongly implicated as a second messenger in early platelet activation. Agonists that cause platelets to change shape and their granules to centralize also lead to an increase in cytoplasmic free calcium (Zavoico and Feinstein, 1984; Hallam et al., 1984; Yoshida et al., 1986). Pretreatment of platelets with phorbol esters before activation by ADP or thrombin inhibits shape change in correlation with the inhibition of the rise in intracellular calcium (Yoshida et al., 1986; Yoshida and Nachmias, 1987). However, agonists cause many other changes, which may require receptor occupancy or other effectors and which are directly caused by increased calcium cannot be determined by correlation. We used saponin permeabilization as a way of increasing calcium levels in the absence of agonist while at the same time allowing soluble proteins to diffuse out, thus greatly improving the structural detail in this very dense cytoplasm.

I. The Structure of the Cytoskeleton

The study of the structural changes taking place in platelets has been difficult. The resting cytoplasm presents as a dense structureless matrix in thin sections and in negatively stained electron micrographs. In such preparations, only short microfilaments can be detected in an amorphous background (Nachmias, 1980; Loftus et al., 1984). However, this appearance is deceptive. The high concentration of soluble proteins, including actin, in these preparations obscures the filaments.

To circumvent this problem, two recent studies made

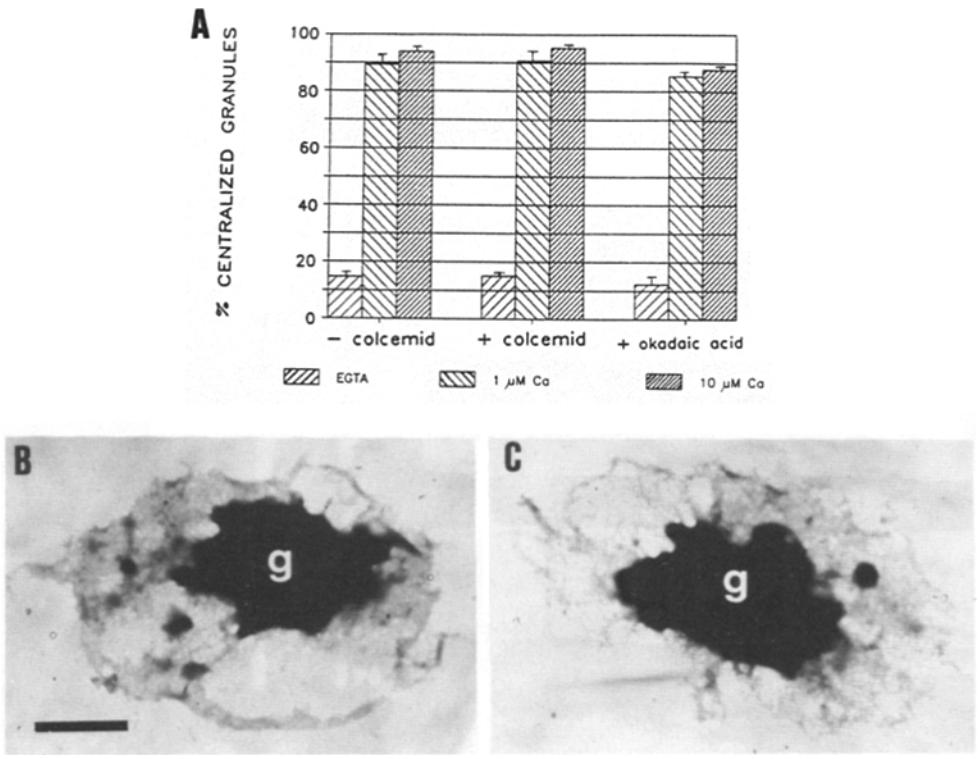

Figure 8. Graph of percentages of platelets permeabilized in the presence of 1 mM ATPγS exhibiting granule centralization with (+ colcemid) or without (− colcemid) prior pretreatment with cold and colcemid to dissociate the microtubule coil. (*A*) Counts of platelets permeabilized in the presence of okadaic acid and 1 mM ATP without cold and colcemid treatment are also shown (+ okadaic acid). Platelets were fixed 15 min after permeabilization and prepared as whole mounts for EM. The results are the means of three experiments for each condition ± SD with 100 platelets scored per experimental condition for each experiment. Note that in the presence of micromolar calcium, >90% of the platelets exhibit centralized granules under all conditions (plus or minus colcemid with ATPγS or with okadaic acid and ATP). The micrographs show whole mounts of platelets permeabilized in 10 μM calcium in the presence of either 1 mM ATPγS (*B*) or 10 μM okadaic acid and 1 mM ATP (*C*). The central area contains the platelet granules (*g*). Bar, 1 μm.

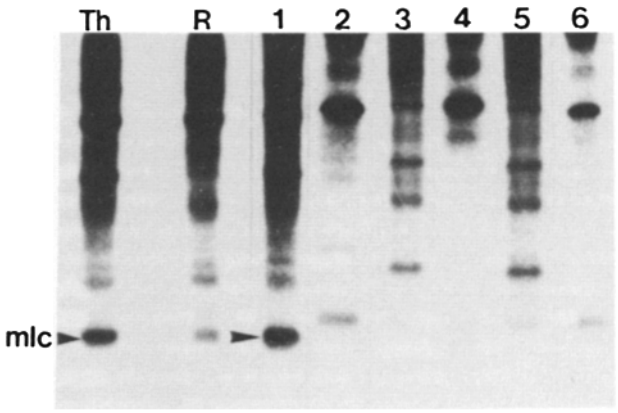

Figure 9. Autoradiograph of a 13% SDS-polyacrylamide gel of platelets permeabilized for 15 min showing phosphorylated myosin regulatory light chain in the presence of micromolar calcium with 10 μM okadaic acid. Platelets were incubated with 1 mCi/ml ^{32}P before permeabilization and 0.25 mCi ATPγ^{32}P, and okadaic acid was added at the time of permeabilization (see Materials and Methods). Intact ^{32}P-labeled platelets with (*Th*) and without (*R*) thrombin stimulation were lysed in SDS-sample buffer for comparison. Lane *1*, cellular fraction of platelets permeabilized in 10 μM calcium and 10 μM okadaic acid; lane *2*, supernatant fraction of platelets in lane *1*; lane *3*, cellular fraction of platelets permeabilized in 5 mM EGTA and 10 μM okadaic acid; lane *4*, supernatant fraction of platelets in lane *3*; lane *5*, cellular fraction of platelets permeabilized in 10 μM calcium alone; and lane *6*, supernatant fraction of platelets in lane *5*. Arrowheads point to the position of myosin regulatory light chain (*mlc*).

platelets permeable so that soluble proteins would diffuse away. Boyles and colleagues (Fox et al., 1984) lysed and fixed platelets simultaneously with Triton X-100 and lysine-glutaraldehyde followed by postfixation with cold osmium tetroxide kept short to avoid breakdown of actin filaments. They found that the resting platelets contained a network of microfilaments, some of which spanned the width of the platelet (~0.5 μm or more). In a second study, Nakata and Hirokawa (1987) centrifuged saponin-permeabilized platelets and examined them by the freeze fracture deep-etch technique. This also showed clear microfilaments. Unlike Boyles' observation, they found bands of microfilaments running circumferentially under the remaining plasma membrane. Because platelets are easily mechanically activated, centrifuging them before fixation might have produced these circumferential microfilaments.

In this study, we permeabilized platelets under controlled conditions designed to minimize activation and fixed them before centrifugation. We do not observe circumferential filaments in platelets permeabilized in EGTA although submembranous filaments are apparent (Fig. 3 *B*). However, we do see circumferential microfilaments partially separated from the membrane in platelets permeabilized in micromolar calcium with (Fig. 6 *B*) or without (Fig. 3, *C–E*) the addition of ATPγS. We also see them in platelets stimulated with ADP and then permeabilized in EGTA (Fig. 4) though these are less dense and are not clearly separated from the membrane. Our findings agree well with those of Fox and

colleagues (1988) on resting platelets and with those of Nakata and Hirokawa (1987) on activated platelets. We suggest that the greater density of the microfilament shells in platelets permeabilized in micromolar calcium may be due to the long (15 min) 1 or 10 μM calcium transient in this permeabilized preparation as compared to the short (<30 s) 0.3–0.6 μM calcium transient following ADP (Yoshida et al., 1986). ADP is known to be a weak agonist in the absence of fibrinogen, i.e., it produces shape change without secretion and it is readily reversible unlike thrombin (Born et al., 1978). Although myosin phosphorylation peaks at 15 s after ADP stimulation, it is rapidly dephosphorylated (Daniel et al., 1984). Therefore, in platelets permeabilized in micromolar calcium, transiently phosphorylated myosin may interact with the F-actin shell long enough to cause partial contraction.

Several earlier studies described packed microfilaments surrounding the granules and separated from the membrane in intact, agonist-stimulated platelets (Gerrard and White, 1976; Carroll et al., 1982). The rings of microfilaments (Fig. 3, *C–E*; Fig. 4, *A–C*) we see also surround the granules. Very similar microfilament rings were reported by Jennings and colleagues (1981) who thin-sectioned pellets of Triton X-100 precipitates of thrombin-activated platelets lysed at 30 sec and 2 min. Their rings, like ours, represent sections through shells since they appear in essentially all of the randomly oriented platelets.

How do these shells of microfilaments form? The possibilities include: (*a*) rapid actin polymerization at selected sites; (*b*) a loss of the links between cytoskeletal components and their membrane connections; (*c*) selective severing of the microfilaments; or (*d*) a combination of the above.

A change in the polymerization state of actin does not seem likely to account for the structural alterations we observe in micromolar calcium. Resting platelets contain ~50–60% G-actin (Fox et al., 1981), and our results agree. We find ~61% G-actin in Triton X-100-treated, resting platelets (Fig. 2). When platelets are stimulated with 0.1 U/ml thrombin, G-actin can fall to 25% of the total actin content in 30 s (Fox, 1986). We do not detect any significant difference in the G-actin diffusing out from platelets permeabilized in either EGTA or micromolar calcium. Under both conditions, the mean concentration of G-actin is between 54 and 58% (Fig. 2). We cannot rule out localized depolymerization and repolymerization of the platelet actin, but we feel it is unlikely because it would have to be so well regulated. The significance of actin polymerization in the formation of the shell of microfilaments and the centralization of the granules in intact, agonist-stimulated platelets remains to be determined.

A second possibility is that links between the membrane and the cytoskeleton are broken. A major link is between plasma membrane-bound glycoprotein Ib and ABP (Fox, 1985; Okita et al., 1985). ABP also cross-links actin filaments (Hartwig and Stossel, 1981; Rosenberg et al., 1981) and is retained in the cellular fractions (Figs. 1 and 5). We do not know if the glycoprotein Ib-ABP link is sensitive to calcium, however, ABP's ability to cross-link actin is not calcium sensitive (Rosenberg et al., 1981). Although its phosphorylation state changes upon platelet activation (Cox et al., 1984), it is still unclear how this affects cross-linking or attachment of microfilaments to the membrane. Proteolysis of ABP by calpain (Fox et al., 1985) is not a factor in our experiments; we always included the inhibitor leupeptin and saw no evidence of proteolysis by gel electrophoresis.

A third possibility is that F-actin is cut near the membrane. Gelsolin is a calcium-activated protein that severs F-actin (Yin and Stossel, 1979; Wang and Bryan, 1981). High-affinity gelsolin–actin complexes form and peak within 15 s after agonist stimulation with thrombin or ADP (Lind et al., 1987), slightly preceding the peak of shape change detected spectrophotometrically (Yoshida et al., 1986). Gelsolin can interact with membrane lipids (Janmey and Stossel, 1987), and Hartwig and colleagues (1989) recently reported that membrane-associated gelsolin increases 15–60 s after exposure to thrombin. Further work is necessary to determine whether gelsolin is involved in severing filaments in these models.

II. Granule Centralization

When platelets are activated, myosin regulatory light chain becomes phosphorylated by a calcium-calmodulin dependent kinase (Dabrowska and Hartshorne, 1978; Hathaway and Adelstein, 1979). Good temporal correlations exist between shape change and phosphorylation of myosin regulatory light chain (Daniel et al., 1984) and between light chain phosphorylation and myosin association with the cytoskeleton (Fox and Phillips, 1982).

In our models when either ATPγS or ATP and okadaic acid is present in addition to micromolar calcium, the cytoskeletal shells decrease to half their original size and become dense, thick masses of microfilaments that surround the centralized granules (Figs. 6 *B*, 8, *B* and *C*). These look remarkably like the structures seen after thrombin activation (Fig. 6 *A*). In the study mentioned above, Jennings and colleagues (1981) found the cytoskeletal rings obtained from platelets treated with thrombin for 2 min were about half the size of those obtained from platelets treated with thrombin for 30 s. Based on the resistance of the thiophosphorylated light chain to phosphatase (Morgan et al., 1976), we assume that ATPγS, like okadaic acid, protects platelet myosin from dephosphorylation during permeabilization. When the light chain is phosphorylated, myosin can interact with actin because phosphorylation increases actin activation of platelet myosin ATPase activity (Adelstein and Conti, 1975), correlates with force production by threads of platelet actomyosin (Leibowitz and Cooke, 1978). Furthermore, the circumferential microfilaments in activated platelets have both polarities so that they could slide to produce a contraction (Nakata and Hirokawa, 1987), and myosin centralizes in thrombin-activated platelets (Painter and Ginsberg, 1984). Thus, platelet myosin, by interacting with the microfilament shell, could cause the centralization of the granules (Figure 8 *B*).

Recent evidence from another nonmuscle system also shows a correlation between myosin light chain phosphorylation and a contractile event. Wysolmerski and Lagunoff (1990) treated monolayer cultures of bovine endothelial cells with agonist and found that the cells retracted their stress fibers towards the nucleus. When they reconstituted saponin-permeabilized endothelial cells with micromolar calcium, calmodulin, myosin light chain kinase, and ATP, the actin

stress fibers also retracted centrally towards the nucleus. When radiolabeled ATPγS was included, myosin light chain thiophosphorylation was seen in correlation with the stress fiber retraction.

We conclude that by retaining myosin phosphorylation, we have induced the microfilament shell in our model system to contract to produce a structure that strongly resembles that seen in thrombin-activated platelets. Although we suspect that myosin filaments are present in the dense mass of microfilaments, they have so far eluded detection. We have tried to visualize such myosin filaments by breaking down the contracted shell mechanically or enzymatically but so far have not succeeded. The state of myosin in these preparations requires further study.

III. The Role of the Microtubule Coil

The role of the microtubule coil in granule centralization has been controversial. White (1969) showed that high levels of colchicine, vincristine or vinblastine caused depolymerization of the microtubule coil and correlated this with the inhibition of ADP-induced granule centralization. However, the alkaloid concentrations used to observe these effects were near toxic levels. Behnke (1970), using a higher concentration of colcemid (1 mM) than our study, observed no inhibition of ADP-induced granule centralization. While White's studies did show granule centralization at lower Vinca alkaloid concentrations and at later stages of platelet aggregation, Behnke's study did not demonstrate the complete loss of the coil in his preparations. Therefore, these studies are inconclusive.

We used cold and colcemid treatment together to ensure depolymerization of the coil before permeabilization and monitored its loss by immunofluorescence. The data indicate that the microtubule coil is not essential for granule centralization. However, there is a subtle difference in the centralized microfilaments of thrombin-treated platelets as compared to those induced in permeabilized platelets: the thrombin-induced structure is more compact and the peripheral contour of the filaments more rounded (Fig. 6). Thus, the microtubule coil might help to shape the contracting mass of microfilaments. While we do not exclude important interactions between the microtubules and the microfilaments either in the maintenance of resting platelet shape or other aspects of cytoskeletal rearrangements, our experiments show that granule centralization can occur very well in the absence of the microtubule coil.

In conclusion, we propose a two-step minimal mechanism for centralization of platelet granules. First, we suggest that the cytoskeletal network is altered in a calcium-dependent manner perhaps losing connections to the membrane cytoskeleton and/or by severing of the microfilaments to form a microfilamentous shell which surrounds the granules. This may account, in part, for the cell body rounding up during platelet shape change. Second, phosphorylated myosin interacts with the actin filaments of the shell to cause contraction and centralization of the granules. In intact platelets, polymerization of actin may also contribute to this proposed mechanism.

The authors would like to thank the following people for their help: Dr. L. Lemanski of State University of New York Syracuse for discussions on whole mount fixation methods; Dr. Avril Somlyo of University of Virginia for the gift of okadaic acid; Drs. R. Hock, J. M. Murray, F. A. Pepe, N. J. Philp, J. W. Sanger, S. Shattil and K. V. Thimann for their discussions and advice during the preparation of this manuscript; and Peggy Yetter for her editorial expertise.

This work was supported by National Institutes of Health (NIH) grant HL-15835 and by NIH training grants HL07502-07 and HL07499.

Received for publication 4 October 1990 and in revised form 15 November 1990.

References

Adelstein, R. S., and M. A. Conti. 1975. Phosphorylation of platelet myosin increases actin-activated myosin ATPase. *Nature (Lond.).* 256:597–598.

Authi, K. S., E. J. Hornby, B. J. Evenden, and N. Crawford. 1986. Inositol 1,4,5-trisphosphate (IP_3) induced rapid formation of thromboxane B_2 in saponin-permeabilized human platelets: Mechanism of IP_3 action. *FEBS (Fed. Eur. Biochem. Soc.) Lett.* 213:95–101.

Behnke, O. 1970. Effect of some chemicals on blood platelet microtubules, platelet shape change and some platelets functions in vitro. *Scand. J. Haematol.* 7:123–140.

Biajolian, C., J. C. Ruegg, and A. Takai. 1988. Effects of okadaic acid on isometric tension and myosin phosphorylation of chemically skinned guinea pig taenia coli. *J. Physiol. (Lond.).* 398:81–95.

Born, G. V. R., R. Dearnly, J. G. Foulks, and D. E. Sharp. 1978. Quantification of the morphological reaction of platelets to aggregating agents and of its reversal by aggregation inhibitors. *J. Physiol. (Lond.).* 280:193–212.

Brass, L. F., and S. K. Joseph. 1985. A role for inositol trisphosphate in intracellular Ca^{2+} mobilization and secretion in platelets. *J. Biol. Chem.* 260:15172–15179.

Carroll, R. C., R. G. Butler, and P. A. Morris. 1982. Separable assembly of platelet pseudopodal and contractile cytoskeletons. *Cell.* 30:385–393.

Chantler, P. D., J. R. Sellers, and A. G. Szent-Gyorgi. 1981. Cooperativity in scallop myosin. *Biochemistry.* 20:210–216.

Cox, A. C., R. C. Carroll, J. G. White, and G. H. R. Rao. 1984. Recycling of platelet phosphorylation and cytoskeletal assembly. *J. Cell Biol.* 98:8–15.

Dabrowska, R., and D. J. Hartshorne. 1978. A Ca^{2+} and modulator-dependent kinase from non-muscle cells. *Biochem. Biophys. Res. Commun.* 85:1352–1359.

Daniel, J. L., I. R. Molish, M. Rigmaiden, and G. Stewart. 1984. Evidence for a role of myosin phosphorylation in the initiation of the platelet shape change response. *J. Biol. Chem.* 259:9826–9831.

Fox, J. E. B. 1985. Identification of actin-binding protein as the protein linking the membrane skeleton to glycoproteins on platelet plasma membrane. *J. Biol. Chem.* 260:11970–11977.

Fox, J. E. B. 1986. Platelet contractile proteins. *In* Biochemistry of Platelets. D. R. Phillips and M. A. Shuman, eds. Academic Press, New York, 115–157.

Fox, J. E. B., and D. R. Phillips. 1982. Role of phosphorylation in mediating the association of myosin with the cytoskeletal structures of human platelets. *J. Biol. Chem.* 257:4120–4126.

Fox, J. E. B., M. E. Docter, and D. R. Phillips. 1981. An improved method for determining the actin filament content of non-muscle cells by the DNase I inhibition assay. *Anal Biochem.* 117:170–177.

Fox, J. E. B., J. K. Boyles, C. C. Reynolds, and D. R. Phillips. 1984. Actin filament content and organization in unstimulated platelets. *J. Cell Biol.* 98:1985–1991.

Fox, J. E. B., D. E. Goll, C. C. Reynolds, and D. R. Phillips. 1985. Identification of two proteins (actin-binding proteins and P235) that are hydrolyzed by endogenous Ca^{2+}-dependent protease during platelet aggregation. *J. Biol. Chem.* 260:1060–1066.

Gerrard, J. M., and J. G. White. 1976. The structure and function of platelets, with emphasis on their contractile nature. *Pathobiol. Annu.* 6:31–59.

Hallam, T. J., A. Sanchez, and T. J. Rink. 1984. Stimulus response coupling in human platelets. *Biochem. J.* 218:819–827.

Hartwig, J. H., and T. P. Stossel. 1981. The structure of actin-binding protein molecules in solution and interacting with actin filaments. *J. Mol. Biol.* 45:563–581.

Hartwig, J. H., K. A. Chambers, and T. P. Stossel. 1989. Association of gelsolin with actin filaments and cell membranes of macrophages and platelets. *J. Cell Biol.* 108:467–479.

Hathway, D. R., and R. S. Adelstein. 1979. Human platelet myosin light chain kinase requires the calcium binding protein calmodulin for activity. *Proc. Natl. Acad. Sci. USA.* 76:1653–1657.

Janmey, P. A., and T. P. Stossel. 1987. Modulation of gelsolin function by phosphatidyl-4,5-bisphosphate. *Nature (Lond.).* 325:362–364.

Jennings, L. K., J. E. B. Fox, H. H. Edwards, and D. R. Phillips. 1981. Changes in cytoskeletal structure of human platelets following thrombin activation. *J. Biol. Chem.* 256:6927–6932.

Kenney, D. M., and R. W. Linck. 1985. The cytoskeleton of unstimulated blood platelets: Structure and composition of the isolated marginal microtubular band. *J. Cell Sci.* 78:1–22.

Leibowitz, E. A., and R. Cooke. 1978. Contractile properties of actomyosin

from human blood platelets. *J. Biol. Chem.* 253:5443–5447.
Lind, S. E., P. A. Janmey, C. Chaponnier, T. J. Herbert, and T. P. Stossel. 1987. Reversible binding of actin to gelsolin and profilin in human platelet extracts. *J. Cell Biol.* 105:833–842.
Loftus, J. C., J. Choate, and R. M. Albrecht. 1984. Platelet activation and cytoskeletal reorganization: high voltage electron microscopic examination of intact and Triton-extracted whole mounts. *J. Cell Biol.* 98:2019–2025.
Morgan, M., S. V. Perry, and J. Ottaway. 1976. Myosin light-chain phosphatase. *Biochem. J.* 157:687–697.
Nachmias, V. T. 1980. Cytoskeletons of human platelets at rest and after spreading. *J. Cell Biol.* 86:795–802.
Nachmias, V. T., J. Sullender, and J. R. Fallon. 1979. Effects of local anesthetics on human platelets: filopodial suppression and endogenous proteolysis. *Blood.* 53:63–72.
Nakata, T., and N. Hirokawa. 1987. Cytoskeletal reorganization of human platelets after stimulation revealed by the quick-freeze deep-etch technique. *J. Cell Biol.* 105:1171–1780.
O'Halloran, T., M. C. Beckerle, and K. Burridge. 1985. Identification of talin as a major cytoplasmic protein implicated in platelet activation. *Nature (Lond.).* 317:449–451.
Okita, J. R., D. Pidard, P. J. Newman, R. R. Montgomery, and T. J. Kunicki. 1985. On the association of glycoprotein Ib and actin-binding protein in human platelets. *J. Cell Biol.* 100:317–321.
Painter, R. G., and M. H. Ginsberg. 1984. Centripedal myosin redistribution in thrombin-stimulated platelets. *Exp. Cell Res.* 155:198–212.
Pollard, T. D., S. M. Thomas, and R. Niederman. 1974. Human platelet myosin. I. Purification by a rapid method applicable to other non-muscle cells. *Anal. Biochem.* 60:258–266.
Rosenberg, S., A. Stracher, and R. C. Lucas. 1981. Isolation and characterization of actin and actin-binding protein from human platelets. *J. Cell Biol.* 91:201–211.
Towbin, H., T. Staehelin, and J. Gordon. 1979. Electrophoretic transfer of proteins from polyacrylamide gels to nitrocellulose sheets: Procedure and some applications. *Proc. Natl. Acad. Sci. USA.* 76:4350–4354.
Wang, L. L., and J. Bryan. 1981. Isolation of calcium-dependent platelet proteins that interact with actin. *Cell.* 25:637–649.
White, J. G. 1969. Effects of colchicine and vinca alkaloids on human platelets. III. Influence on primary internal contraction and secondary aggregation. *Am. J. Pathol.* 54:467–478.
Wysolmerski, R. B., and D. Lagunoff. 1990. Involvement of myosin light chain kinase in endothelial cell retraction. *Proc. Natl. Acad. Sci. USA.* 87:16–20.
Yin, H. L., and T. P. Stossel. 1979. Control of cytoplasmic actin gel-sol transformation by gelsolin, a Ca^{2+}-dependent regulatory protein. *Nature (Lond.).* 281:583–586.
Yoshida, K., and V. T. Nachmias. 1987. Phorbol ester stimulates calcium sequestration in saponized human platelets. *J. Biol. Chem.* 262:16048–16054.
Yoshida, K., G. Dubyak, and V. T. Nachmias. 1986. Rapid effects of phorbol ester on platelet shape change, cytoskeleton and calcium transient. *FEBS (Fed. Eur. Biochem. Soc.) Lett.* 206:273–278.
Yoshida, K., F. Stark, and V. T. Nachmias. 1988. Comparison of the effect of phorbol 12-myristate 13-acetate and prostaglandin E_1 on calcium regulation in human platelets. *Biochem. J.* 249:487–493.
Zavoico, G. B., and M. G. Feinstein. 1984. Cytoplasmic Ca^{2+} in platelets is controlled by cyclic AMP: Antagonism between stimulators and inhibitors of adenylate cyclase. *Biochem. Biophys. Res. Commun.* 120:579–585.